Journal of Hydrology 610 (2022) 127848

Contents lists available at ScienceDirect

Journal of Hydrology

journal homepage: www.elsevier.com/locate/jhydrol

Research papers

Stable isotope variability of precipitation and cave drip-water at Jumandy cave, western Amazon River basin (Ecuador)

Angie Jiménez-Iñiguez [a], Angela Ampuero [b], Bryan G. Valencia [a], Victor C. Mayta [c], Francisco W. Cruz [b], Mathias Vuille [d], Valdir F. Novello [e], Nicolás Misailidis Stríkis [b], Nataly Aranda [a], Bruno Conicelli [a,*]

[a] Facultad de Ciencias de la Tierra y Agua, Universidad Regional Amazónica Ikiam, Km 7, vía Muyuna, Tena, Napo, Ecuador
[b] Institute of Geosciences, University of São Paulo, São Paulo 05508-080, Brazil
[c] Department of Atmospheric and Oceanic Sciences, University of Wisconsin, Madison, WI, USA
[d] Department of Atmospheric and Environmental Sciences, University at Albany, 1400 Washington Avenue, Albany, NY 12222, USA
[e] Department of Geosciences, University of Tübingen, Germany

ARTICLE INFO

This manuscript was handled by Huaming Guo, Editor-in-Chief, with the assistance of Prosun Bhattacharya, Associate Editor

Keywords:
Karst
Stable isotopes
Paleoclimatic reconstructions
Amazon
Amount effect

ABSTRACT

Monitoring studies are necessary to better understand the hydrological processes affecting the isotopic signature of cave waters, which are ultimately recorded in speleothems that are used as paleoclimate archives. This research examines changes in the isotopic composition ($\delta^{18}O$ and $\delta^{2}H$) of precipitation as it infiltrates through the epikarst and into the Jumandy cave, located in the western Amazon Basin (Ecuador). Meteorological and hydrological parameters were monitored outside and inside the cave, and isotope analyses were carried out in waters from rainfall, an underground river, and drip-water at two sampling sites in the cave between April 2019 and February 2020. At monthly timescale, the rainfall weighted isotopic composition monitored at our stations was strongly correlated with the mean precipitation amount. However, when considered at weekly time-steps, the correlation is only moderate. This implies that the variation of the isotopic composition in the study area cannot be interpreted exclusively as an amount effect. Isotopic values and back-trajectory modeling show that the isotopic signature was affected by the moisture source effect associated with upstream rainout. The moisture flux is dominantly from an east to northeast direction and moisture mainly originates over the Atlantic Ocean, passing through the Amazon Basin. A significant fraction of moisture is associated with local sources within the Amazon Basin. This aspect is confirmed by d-excess values of rainfall and the Local Meteoric Water Lines (LMWLs) that indicate an influence of the high evapotranspiration rate of the Amazon region on the isotopic composition of local rainfall. The infiltrated water resides for about three weeks in the epikarst and then precipitates forming speleothems (residence time). However, this short residence time needs to be confirmed with a longer monitoring period. Despite the different magnitudes of the dripping rates, the isotopic values at the two monitored sites are similar. This suggests that the dripping discharge rate is affected by the karst structure, but the isotopic signature reflects the mixing of individual rainfall events above the cave. Therefore, $\delta^{18}O$ in speleothems from these caves is mainly recording short-term precipitation changes linked to regional and large-scale atmospheric circulation.

1. Introduction

Solutes dissolved in percolated water, such as calcium carbonate, dripping in cave environments, allow for the formation of speleothems that grow in layers over time as carbonate precipitates (Luo et al., 2013). As they grow, the speleothems retain the isotopic signature of the percolated rainwater within the carbonate layers (Clark, 2015). Thereby, these structures provide high-resolution records, capable of retaining the isotope variability of the rainfall at interannual time-scale, allowing us to reconstruct past climatic variability (Fairchild et al., 2006; Fuller et al., 2008; Matthews et al., 2000; Rozanski et al., 1997; Wainer et al., 2011).

* Corresponding author.
E-mail address: bconicelli@gmail.com (B. Conicelli).

https://doi.org/10.1016/j.jhydrol.2022.127848
Received 6 January 2022; Received in revised form 21 March 2022; Accepted 16 April 2022
Available online 22 April 2022

The rainfall isotopic variations in tropical regions result from the combined effect of altitude, rainfall amount, moisture source, and Rayleigh distillation (Gat and Matsui, 1991; Grootes et al., 1989; Rozanski et al., 1993). The altitude effect consists of progressive isotopic depletion due to orographic uplift and condensation of water vapor (approximately −2 to −3 ‰ of $\delta^{18}O$/km) (Gonfiantini et al., 2001), as the uplift leads to cooling, condensation and preferential removal of the heavier isotopes, thereby rendering the remaining water vapor increasingly more depleted in heavy isotopes at higher elevations (Hurley et al., 2016). In tropical South America, oxygen isotopic ratios in speleothems are mainly reflecting the degree of rainout upstream associated with Rayleigh distillation during transport (Dansgaard, 1964); hence they record changes in monsoon dynamics and convective activity over the Amazon Basin (Campos et al., 2019; Grootes et al., 1989; Vimeux et al., 2005; Vuille et al., 2012), the amount of precipitation (*amount effect*) (Moquet et al., 2016) and changes in moisture source (*source effect*) (Lee et al., 2009). The amount effect is dominant in areas close to the moisture source such as in coastal areas (Craig and Gordon, 1965; Lachniet, 2009). In the Peruvian Amazon and the Andes, on the other hand, the long-range transport from source to sink lead to progressive loss of heavy isotopes along the moisture pathway and therefore a stronger imprint of the degree of rainout upstream, reflecting large-scale monsoon dynamics (Vimeux et al., 2005; Vuille et al., 2003; Vuille et al., 2012). On the other hand, the source effect dictates the origin and trajectory of an air mass linked to processes of evaporation, relative humidity, and degree of rainout upstream (DRU), that influence the isotopic signature at the ultimate precipitation site (Ampuero et al., 2020; Kanner et al., 2013; Vimeux et al., 2005; Vuille and Werner, 2005). DRU refers to the amount of precipitation upstream, integrated along the trajectory of an air mass. Therefore, far from the moisture source, the isotopic composition of rainfall is not a straightforward function of the local rainout, instead, it reflects the history of the convective processes that occurred along the atmospheric moisture transport pathway. This factor is relevant to the interpretation of isotope records in the Andes.

The isotopic signature measured in the cave drip-waters may differ from the one originally observed in rainfall due to multiple processes acting in the soil, epikarst and fractures in the transmission zone (Constantin et al., 2018; Dhungana and Aharon, 2019), which have implications to the isotopic signature recorded in the speleothem carbonate (Dreybrodt and Scholz, 2011; Fairchild et al., 2006). Cave drip waters reflect a long-term weighted mean of the isotopic composition of precipitation (Chapman et al., 1992; Moquet et al., 2016; Williams and Fowler, 2002; Yonge et al., 1985) and paleoclimate reconstructions based upon speleothems require adequate calibration, as the fractionation processes are site-specific (Duan et al., 2016). Therefore, ensuring a modern understanding of the processes that may alter the isotopic composition in a speleothem is key to calibrate the proxy archive for reconstructing past rainfall variability, temperature changes, or atmospheric circulation at various timescales (Cobb et al., 2007; Dhungana and Aharon, 2019; Lambert and Aharon, 2010; Polk et al., 2012).

In the Amazon Basin the study of climate controls on isotopic variability and how they related to hydroclimate, and atmospheric circulation, are limited. The few existing studies indicate that, over continental areas, DRU explains a significant fraction of the observed variance in the isotopic composition of rainfall on weekly to monthly timescales (Ampuero et al., 2020; Della Libera et al., 2022; Kanner et al., 2013; Villacís et al., 2008; Vimeux et al., 2005; Vuille and Werner, 2005). In contrast, the meaning of the speleothem isotope records from areas covered by Amazon Forest at the Andes foothills is not fully understood (Cheng et al., 2013; Mosblech et al., 2012). A more recent study has attributed the differences in $\delta^{18}O$ variability across the basin to be a function of the relative contribution from local recycled moisture from evapotranspiration versus transported moisture from distal sources in the tropical Atlantic, where the first source dominates over areas in the western Amazon (Wang et al., 2017). Mosblech et al. (2012) performed a paleoclimate study over the last 100 kyrs using four stalagmites from Santiago cave (Ecuadorian Amazon) and established that the past recorded history of rainfall in this part of the Amazon was controlled by the North Atlantic Oscillation (NAO). However, since this study was not calibrated with local information, does not account for the possible influence of other regional and local effects.

The present study seeks to analyze the relationship between isotopic variability in modern rainfall, drip-water, and water from river drainages inside the Jumandy cave, located in the westernmost part of the Amazon River basin. The results of a weekly monitoring program are reported for the period from April 2019 to February 2020, and compared with meteorological variables and the transport history of air masses to determine the most relevant controls on the isotopic signature of rainfall. This investigation allows for a more detailed understanding of the cave environment and provides a reference to calibrate paleoclimate studies in this region.

2. Study area

Two rainfall collecting sites were surveyed for isotopic analysis, one at Universidad Regional Amazónica Ikiam represented as Ikiam station (0°57′ S, 77°51′ W; 610 m) and the other at the Jumandy cave entrance referred to as Jumandy station (0°52′ S, 77°47′ W; 650 m), located in western Amazon Basin, in the Napo province, Ecuador (Fig. 1). The cave lies in the Napo Formation, which consists of Cretaceous marine limestones interbedded with shales that were uplifted during the Cenozoic (Estupiñan et al., 2010; Hoorn et al., 2010). Limestone formations cover about 5–10 % of Ecuador's surface area (283.560 km^2) and their outcrops lead to the formation of karst aquifers, mostly in the Amazon Basin (Constantin et al., 2018). The Jumandy cave was formed by the dissolution of the 70–90 million-year-old limestones that belong to the Napo karst system (Sánchez et al., 2017). The cave has a length of 2 km and has a narrow entrance of 2 m that connects to several branches and an underground river called Lluya Yaku that flows permanently inside the cave (Bauz and Mena, 2015). The monitoring took place at 550 and 1500 m distance from the cave entrance, respectively (Fig. 2). The average thickness of the epikarst is 8.6 m, and the strata that constitute the vadose zone are unconsolidated material, limestone rocks, highly fractured limestone rocks, and limestone bedrock (Rivera, 2022).

Climatological information recorded at Archidona station (0°55′ S, 77°49′ W; at 2.6 km distance from the study area) from 2001 to 2014 indicates a mean annual precipitation and temperature of 4091 mm and 23.9 °C, respectively. This region is close to the equator; therefore it receives more of its precipitation associated with the annual march of convective activity over the site which occurs twice a year, in March to May (Espinoza et al., 2009). The percentage of annual precipitation recorded in austral winter (June-July-August, JJA) and spring (September-October-November, SON) was 27 % and 23 % respectively. The lowest precipitation amount (20 %) fell in austral summer (December-January-February, DJF) with minimum of –233 mm/month recorded in January and the highest precipitation (29 %) in autumn (March-April-May, MAM). The precipitation is quite equally distributed around the year, as one would expect for a site located so close to the equator. The mean annual cycle of air temperature in the Amazon Basin shows that highest temperatures are reached ahead of the rainy season. Once convective cloud cover builds up during the rainy season, the surface receipt of solar radiation is reduced, thereby lowering temperature at the surface (Garreaud et al., 2009).

3. Methods

Due to the Coronavirus pandemic (COVID-19), the study was interrupted from March to December 2020 and was resumed in January 2021. There is a four-week gap included in the monitoring period, due to bad weather conditions and a National Protest in Ecuador in October 2019. In the weeks where sampling did not occur, the drip volume and

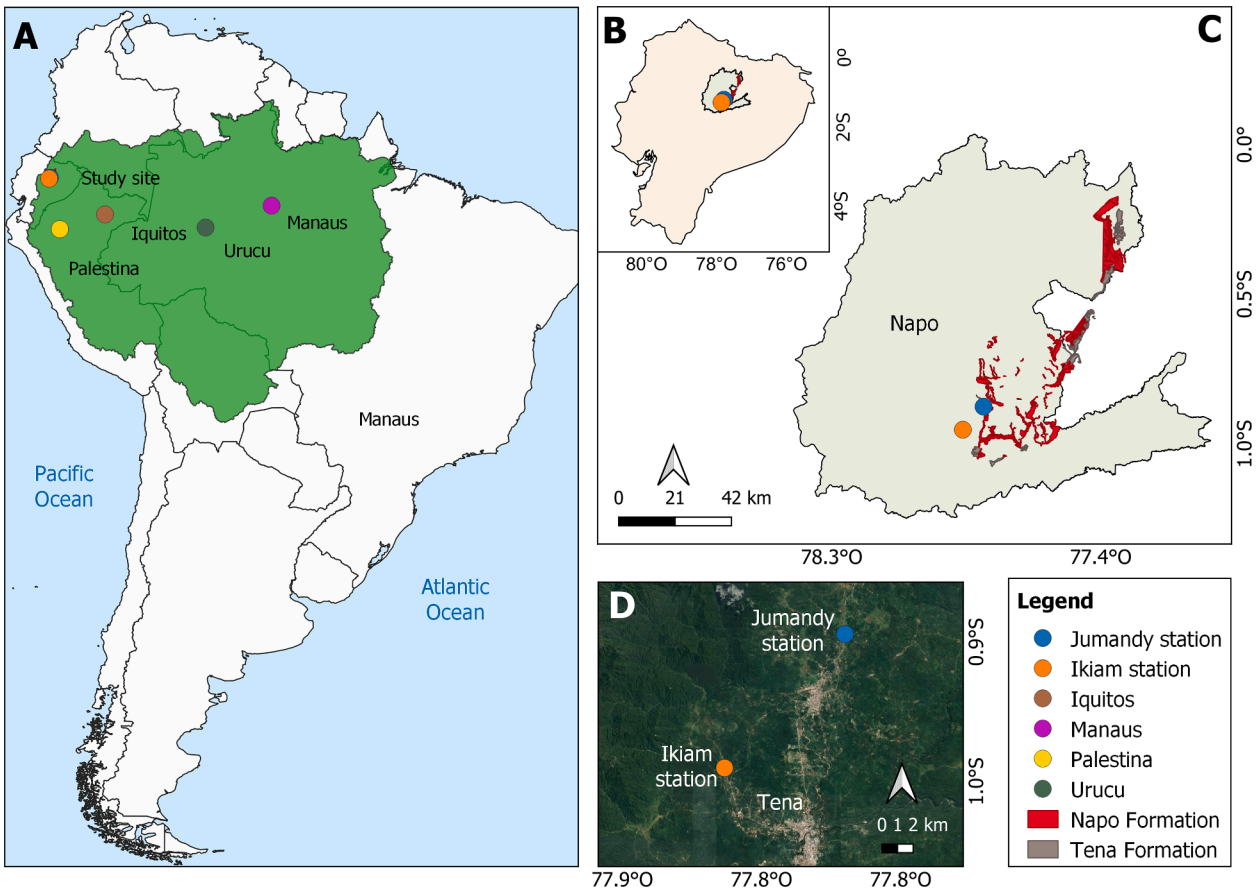

Fig. 1. Map of study site. A) The stations: Iquitos, Manaus, Urucu, Palestina, and study site. B) Location of Napo province in Ecuador. C) Napo province with Napo and Tena geological formations. D) Locations of Ikiam and Jumandy stations where meteorological measurements and sampling of isotopic composition of rainfall were monitored.

the isotopic composition were accumulated for 15 days. The weekly relative drip-rate was then determined based on the drip volume and the monitoring time. The drip-water isotopic data were plotted on the Local Meteoric Water Line (LMWL) and Global Meteoric Water Line (GMWL), which indicated that there is no significant difference between the isotopic signature accumulated during 15 and 7 days.

No outliers were discarded, as they were considered representing reasonable observations of an unusual climatic situation. The statistical procedures applied were: 1) Spearman correlation (ρ) to detect significant relationships between the meteorologic and isotopic variables. This coefficient was considered because it is range-based and robust to the influence of outliers. 2) Simple linear regression to build the LMWLs. 3) ANOVA to compare the regression lines (LMWLs) and detect if there are significant differences between the intercepts and slopes.

3.1. Monitoring outside the cave

Rainwater samples were collected weekly (42 weeks) for isotopic analyses employing two rain-gauges located at Ikiam and Jumandy stations following the protocols of IAEA/WMO (2014) (https://www.iaea.org/). The rain-gauges consisted of a funnel connected to a 4 L tank placed inside a reflective white box to avoid thermal changes that could lead to evaporation and isotopic fractionation during rainfall collection. The water from the tank was mixed and stored in 60 mL air-tight amber glass bottles avoiding air bubbles. The samples were kept refrigerated at 4 °C prior to isotopic analysis. The meteorological variables were recorded with an automatic meteorological station at the Ikiam site (https://meteorologia.ikiam.edu.ec/) and a Data-Logging Rain Gauge RG3-M with a calibration accuracy of ± 1.0 % (0.2 mm measurement increments) installed above the Jumandy station. The variables recorded were precipitation, air temperature and relative humidity.

3.2. Cave monitoring

The drip-water gauges (DW1 and DW2) were installed inside the Jumandy cave following the methodology described by Dhungana and Aharon (2019). Each gauge consists of a funnel of 0.1 m diameter connected directly to a 1 L hermetic plastic bag that stores the percolating water from an active stalactite. Water from cave drainage was collected at two locations as depicted in Fig. 2 (WF1 and WF2) to compare the isotopic composition in the main drainage and its tributary. The samples were collected weekly in amber glass bottles of 60 mL sealed without headspace and refrigerated at 4 °C until analysis.

Two onset Hobo Pro v2 data loggers (accuracy: ± 0.21 °C from 0 to 50 °C; resolution: 0.02 °C at 25 °C) were installed at 300 and 1500 m distance from the entrance of the cave to measure the air temperature and relative humidity every 10 min to check the climate variability in the cave (Fig. 2). These records were converted to weekly averages to match the temporal resolution of the isotopic water sampling. To determine the dripping discharge rates for the speleothems and investigate the flow characteristics of the water that infiltrates in the epikarst, the time it takes to fill a known volume was calculated weekly. Also, the water level of the river inside the cave was measured to determine the water fluctuation in real-time using the HOBO U20L Water Level Data Logger (resolution: < 0.014 kPa). The water level (H) was used to calculate the flow or runoff (Q) within the cave applying the Q-H curve on a daily time-scale.

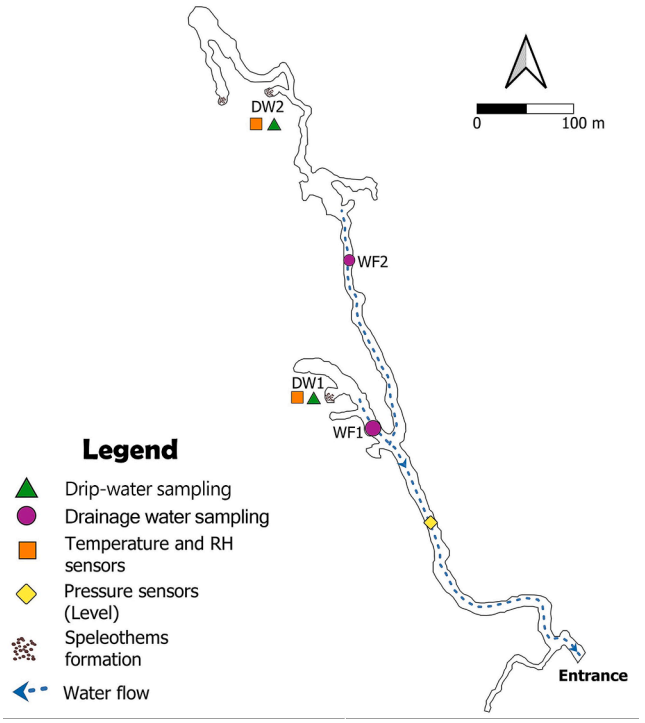

Fig. 2. Jumandy cave map depicting the monitoring sites. The cave has two main branches with three speleothem formation sites (brown dots) of which two have been monitored. Green triangles represent the locations of the two dripping-water gauges (DW1 and DW2). The violet circles represent sites where the underground drainage was sampled (WF1 and WF2). Orange squares represent the HOBO sensors located near drip-water gauges to record the air temperature and relative humidity. The pressure sensors are located at 300 m of the cave entrance (yellow rhombus). The water flow of the stream is to the northeast of the Jumandy cave (blue dash line). Modified from Sánchez et al. (2017).

3.3. Stable isotope analysis

The isotopic composition of 252 water samples was analyzed for hydrogen and oxygen (δ^2H and $\delta^{18}O$) in rainfall (n = 84), drip-water (n = 84), and cave drainage (n = 84). Samples with solid debris were sifted with a 0.45 μm mesh diameter cellulose filter. The analysis was conducted in the Laboratorio Nacional de Referencia del Agua (LNRA) at the Universidad Regional Amazónica Ikiam, using Laser Spectroscopy (Los Gatos Research LWIA – 45 EP). Water samples were processed according to IAEA/WMO (2014) protocols with standards obtained at different heights within Ecuador. The standards used in the study were validated by IAEA and are listed in Supplementary material: Table A.1. Results are expressed in parts per mil (‰) relative to the international isotopic measurement standard Vienna Standard Mean Ocean Water (V-SMOW), with an analytical precision of ± 0.1 ‰ for $\delta^{18}O$ and ± 0.3 ‰ in the case of δ^2H. The monthly weighted average for precipitation and deuterium excess were also calculated (Supplementary material: Text A.2).

3.4. Back-trajectory model

Seven-day air parcel back-trajectories were computed with the HYSPLIT 5.1 model (HYbrid Single-Parcel Lagrangian Integrated Trajectory 5.1) (Rolph et al., 2017; Stein et al., 2015) using ERA 5 data on pressure levels (Hersbach et al., 2018a) and at the surface (Hersbach et al., 2018b) in 0.75° x 0.75° resolution (~80 km). Back-trajectories were initiated at the Ikiam station, at the height of 1000 m above ground level (~730 hPa), within the lower atmospheric layer where the most significant moisture transport to the study site takes place. They were simulated once a day over the monitoring period, accounting only for the back-trajectories that initiate on precipitation days at the Ikiam station. Although this period is too short to describe the climatology, we consider it appropriate to illustrate the source variability during the observation period (for more details about the calculations see Supplementary material: Text A.3). Due to the proximity of the monitoring stations (about 10 km), back-trajectory simulations are performed only at the Ikiam station, as computations at Jumandy station would lead to very similar results. To obtain the representative patterns of the back-trajectories and assess their frequency and timing, a cluster analysis was performed. The Hierarchical Clustering Analysis algorithm with Squared Euclidean distance from the HYSPLIT was applied. To further assess these results, we compared the clusters with composites of the regional anomalies of precipitation and vertically integrated moisture flux.

3.5. Degree of rainout upstream (DRU)

Precipitation along the moisture transport pathway, often referred to as degree of rainout upstream (DRU) is a major control on the isotopic composition of precipitation in continental locations where precipitation results from large-scale moisture transport. We estimated DRU by pairing GPM daily precipitation with the calculated back-trajectories, and accumulated precipitation along the back-trajectory up to the monitoring site. Only precipitation over the continent was considered.

To compare DRU with the isotopic data, we calculated weighted mean values using the local precipitation amount observed at the Ikiam station. Thereby, we account more accurately for the contribution of each precipitation event with a unique DRU value, to the monitored isotopic signature of precipitation.

4. Results and discussion

4.1. Isotopic composition of rainfall

The meteorological variables and isotopic composition of rainfall recorded at Jumandy and Ikiam stations indicate that they behave very similarly as they fluctuated mostly in-phase on a weekly basis (Fig. 3). The δ^2H and $\delta^{18}O$ of precipitation are closely correlated ($\rho = 0.99$; p-value < 0.01) at both stations. The isotopic rainfall samples ranged from −16.9 to 1.0 (‰) for $\delta^{18}O$ and from −124.1 to 17.8 (‰) for δ^2H at Jumandy station; and from −16.5 to 0.3 (‰) for $\delta^{18}O$ and from −122.8 to 10.8 (‰) for δ^2H at the Ikiam station. The mean $\delta^{18}O$ and δ^2H values at Jumandy station were −6.4 and −38.3 (‰) respectively, whereas at Ikiam station they were −5.8 and −34.2 (‰) (Fig. 3C and D). Monthly values of $\delta^{18}O$ at Ikiam and Jumandy stations were estimated through means weighted by the amount of rainfall. The depleted monthly $\delta^{18}O$ values at Ikiam and Jumandy stations coincide with the highest precipitation amounts (Fig. 4). The $\delta^{18}O$ timeseries at the study site were compared with two nearby sites in the Amazon Basin available in the Global Network of Isotopes in Precipitation (GNIP) database hosted within the IAEA (Fig. 4B) and with data from two independent studies. IAEA stations included were: Manaus (3.70°S, 60.10°W, data from 1965 to 1999) and Iquitos (3.49°S, 73.22°W, data from 2006 to 2012), located in Brazil and Peru, respectively. The other records were published as part of a study conducted by Ampuero et al. (2020) from 2012 to 2018 at the Palestina station (5.92°S, 77.35°W) in the Peruvian Amazon and a stable isotopes study carried out by Souza et al. (2015) from 2008 to 2009 in the Urucu Oil Province (4.52°S, 65.18°W) in the Brazilian Amazon. The mean $\delta^{18}O$ value from the Palestina station (−6.59 ‰), Urucu (−6.36 ‰) and Iquitos-GNIP station (−5.72 ‰) feature similar values as Ikiam (−5.7 ‰) and Jumandy (−6.3 ‰) stations. On the other hand, the most eastern station is characterized by less depleted values (Manaus, −4.07 ‰), due to a shorter distance to the moisture source in the Atlantic (reduced Rayleigh fractionation). The most negative values are recorded in the periods of March-June and October-December

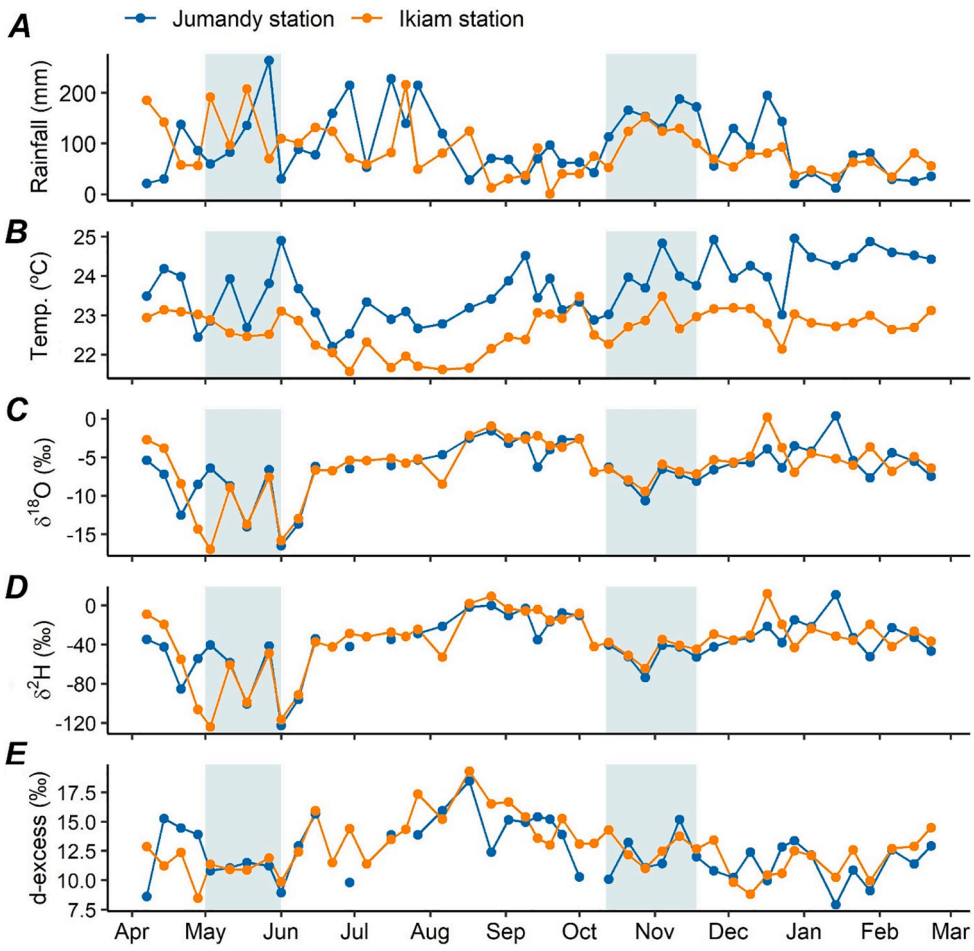

Fig. 3. Isotopic monitoring of rainfall and meteorological variables. The monitoring was realized at Jumandy station (blue color) and Ikiam station (orange color) on a weekly time scale. A) Rainfall amount. B) Air temperature. C) $\delta^{18}O$ values of rainfall. D) $\delta^{2}H$ values of rainfall. E) d-excess values of rainfall. The light blue rectangles denote the two periods where samples of $\delta\ ^{18}O$ dropped below −10 ‰. In addition, note the absence of isotopic data during the four weeks that were not monitored (one week in June, two weeks in July and one in October) at Jumandy station.

(Fig. 4B). The ANOVA results show that the means of the isotopic values were similar between all stations and the information reported in this study ($F = 1.32$; p-value = 0.269). This means that despite the difference in the monitoring time, the seasonality of the monthly mean isotopic composition did not change.

For Jumandy station, the $\delta^{18}O$ and $\delta^{2}H$ values of rainfall display a moderate negative correlation with the weekly precipitation amount, significant at the 95 % level ($\rho = -0.39$ and $\rho = -0.38$, respectively; Table 1). In comparison a higher correlation, significant at 99 % level is observed between $\delta^{18}O$ and $\delta^{2}H$ values with precipitation accumulation at Ikiam station ($\rho = -0.51$ and $\rho = -0.50$ respectively; Table 1). The rainfall amount effect is more strongly observed on monthly, intra-seasonal, or interannual time scales than in weeks, days, or hours (Risi et al., 2008; Rozanski et al., 1993). In the Jumandy cave, the correlation of rainfall amount and isotopic data, taken at weekly timescales, explained 15 % of the variance. However, when the temporal weighting for the isotopes of precipitation shifted from weekly to monthly values, the correlation increased ($\rho = -0.65$; p-value = 0.03), which means that 42 % of the variance was explained. In a study carried out at Cajas in the southwest of Ecuador a moderate correlation between $\delta^{18}O$ and rainfall amount on a weekly scale ($r = -0.37$; p-value < 0.01) and a strong one a monthly scale ($r = -0.60$; p-value < 0.01) were found (Esquivel-Hernández et al., 2019). This large unexplained variance in the short-term variations is a consequence of processes that were omitted in the regression analysis, such as convection, cloud microphysics, cloud types, and humidity transport that affect the isotopic composition of rainfall (Aggarwal et al., 2016; Hastenrath, 1997). These processes are included when calculating monthly means, despite not being directly controlled by rainfall amount, but by factors mentioned above (Hoffmann, 2003; Villacís et al., 2008; Vimeux et al., 2005). Therefore, the weekly monitoring scale of this study allows for a better perspective of the physical convective processes that influence the isotopic signature compared to those accumulated over periods of months.

The parameters that control the rainfall isotopic composition in tropical areas have not been fully understood due to the limited spatial coverage and temporal resolution of the available data (Hoffmann, 2003; Vuille, 2018). The amount effect is expected to be significant in places closer to the moisture source, as long as no long-range transport has occurred. Studies carried out in the tropics (Munksgaard et al., 2019), especially those performed in South America (Gastmans et al., 2017; Salati et al., 1979; Souza et al., 2015; Vimeux et al., 2005) including the Amazon Basin in Ecuador (Windhorst et al., 2013) show that isotopic variability is associated primarily with regional, rather than local, upstream convective activity. Consequently, $\delta^{18}O$ values in this study site are not solely controlled by the amount effect, but, by moisture source effects and the transport history (condensation, rainout, and mixing with air masses that have undergone evapotranspiration) of air masses (Wang et al., 2017). The $\delta^{18}O$ values did not increase when precipitation declined at the end of rainy season, during the first and second week of June, when the $\delta^{18}O$ values remained very negative, reaching values of −16.7 and −13.6 (‰), even though rainfall remained below 100 mm. One explanation for these values is that at the end of the rainy season, precipitation is fueled by moisture that is very depleted in ^{18}O reflecting the end of intense convection upstream over the Amazon Basin. This delayed effect was documented over the Peruvian Andes by Hurley et al (2015). Hence, at the end of the rainy season highly depleted moisture produces lighter than expected $\delta^{18}O$ values, even for small accumulation events.

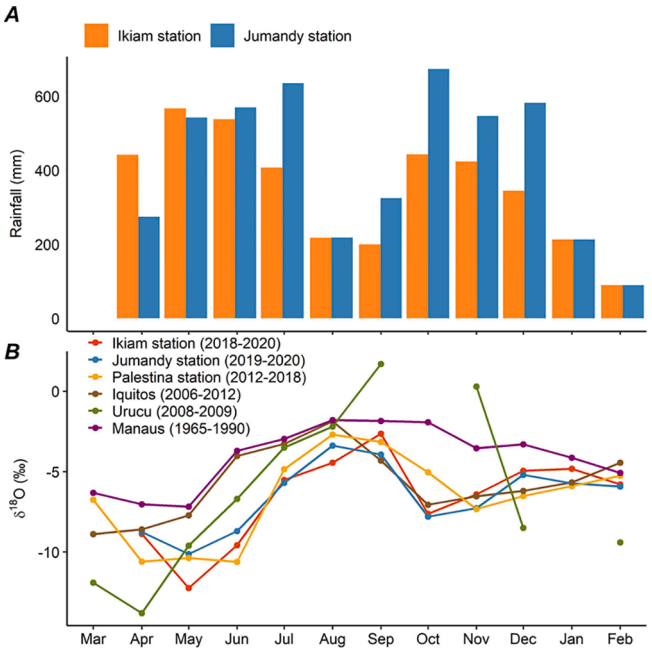

Fig. 4. Behavior from $\delta^{18}O$ of rainfall in relation to precipitation. A) Monthly record of precipitation at Jumandy station (blue bars) and Ikiam station (orange bars). B) Variation of $\delta^{18}O$ at stations located in the Amazon basin at Palestina (yellow dot-line) and Iquitos (brown dot-line), located in Peru; Urucu (green dot-line) and Manaus (purple dot-line), located in Brazil; Ikiam station (orange dot-line) and Jumandy station (blue dot-line) of this study in Ecuadorian Amazon. The $\delta^{18}O$ values at Palestina, Ikiam, and Jumandy station represent monthly means, weighted by the amount of rainfall, while the others are monthly mean GNIP values. $\delta^{18}O$ values of rainfall have bimodal behavior that is impoverished between March-June and September-November.

There is a weak negative correlation between the $\delta^{18}O$ values of rainfall and air temperature (T) and relative humidity (RH), both at Jumandy station (T: $\rho = -0.02$; RH: $\rho = -0.12$) and Ikiam station (T: $\rho = -0.05$; RH: $\rho = -0.04$); none of these correlations are significant at the 95 % level (Table 1). This indicates that the temperature effect does not influence the $\delta^{18}O$ variations of the local rainfall on short timescales, which is consistent with previous studies in the Andes (Vuille et al., 2003; Hardy et al., 2003). The study site experiences a mean annual temperature of 23 °C that increases by 1 °C in August and September, therefore the lack of a significant temperature-relationship is entirely consistent with its very low seasonal amplitude. Also, there was no correlation, significant at the 95 % level, between weekly d-excess and temperature at Jumandy station ($\rho = -0.19$; Table 1), but there was a moderate correlation, significant at the 99 % level, between d-excess and temperature at Ikiam station ($\rho = -0.45$; Table 1). This means that the seasonal temperature variation in the study area is just too low to imprint any significant isotope effect in rainfall but it could leave an imprint in the d-excess. However, the monitoring time is too short to draw any firm conclusions.

The monthly precipitation-weighted isotopic values were used to construct the LMWLs which were plotted together with the GMWL (Fig. 5). The LMWL of Jumandy and Ikiam stations are: $\delta^2H = 8.30 \pm 0.10\ \delta^{18}O + 14.64 \pm 0.33$, n = 42 and $\delta^2H = 8.33 \pm 0.20\ \delta^{18}O + 14.65 \pm 1.28$, n = 42, respectively. The slopes of the LMWLs from Jumandy station (8.30) and the Ikiam station (8.33) overlap and are consistent with the GMWL slope (8.0). The LMWLs intersections of Jumandy station (14.64) and the Ikiam station (14.65) are higher than the global average value of 10 (Fig. 5). In comparison, the LMWLs from other nearby places in the Amazon Basin were $\delta^2H = 8.40\ \delta^{18}O + 16.74$ for Palestina station, $\delta^2H = 8.50\ \delta^{18}O + 13.65$ for Iquitos, $\delta^2H = 7.96\ \delta^{18}O + 10.25$ for Urucu, and $\delta^2H = 8.14\ \delta^{18}O + 12.96$ for Manaus station. The intercept values from the LMWLs (d-excess) presented here are slightly above of the range of 9.80 to 14.60 (‰) proposed by Salati et al. (1979) as typical values in precipitation resulting from air masses that cross the Amazon. It can be attributed to the reduced recycling and to secondary processes of re-evaporation and mixing of air masses that move across the Amazon and precipitate in the local area (Dhungana and Aharon, 2019; Rozanski et al., 1993). A study conducted by Staal et al. (2018) established that 32 % of rainfall over the Amazon Basin is produced by total evapotranspiration. The Amazon rainforest reintroduces heavy isotopes into the atmospheric vapor (recycled moisture) where $\delta^{18}O$ values of these air masses are thereby enriched in heavy isotopes (Gat and Matsui, 1991; Martinelli et al., 1996; Villacís et al., 2008). D-excess allows evaluating the extent of moisture recycling (Araguás-Araguás et al., 2000; Froehlich et al., 2002; Gat and Matsui, 1991; Salati et al., 1979). At Jumandy station, the monthly average values of d-excess

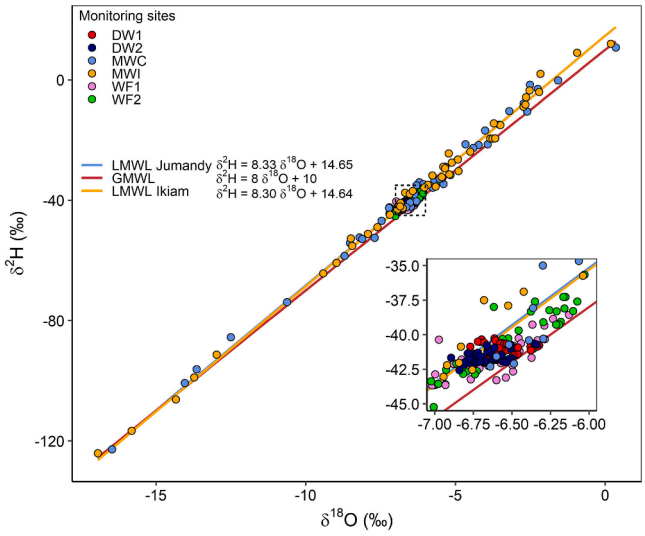

Fig. 5. Scatter plot of $\delta^{18}O$ and δ^2H in precipitation, cave drip-water, and water from river drainages. LMWL of Jumandy station (blue line) and Ikiam station (orange line) plotted in relation to the GMWL (red line). Shown are the values of $\delta^{18}O$ and δ^2H of drip-water at site 1 (DW1, red dots), site 2 (DW2, dark blue dots), of meteoric water at Jumandy station (MWC, blue dots) and at Ikiam station (MWI, orange dots), and of water from river drainages at site 1 (WF1, pink dots) and at site 2 (WF2, green dots). Central part of this graph (dashed box) is enlarged for clarity.

Table 1
Spearman's correlations between isotopic values from rainfall and meteorological variables. $\delta^{18}O$ and δ^2H in relation to temperature ($\delta^{18}O$ - T, δ^2H - T), precipitation ($\delta^{18}O$ - P, δ^2H - P), and relative humidity ($\delta^{18}O$ - RH, δ^2H - RH) and the correlation between temperature and d-excess (T – d-excess) on the weekly time scale.

Stations	*Temperature*			*Precipitation*		*Relative humidity*	
	$\delta^{18}O$	*δ^2H*	*d-excess*	*$\delta^{18}O$*	*δ^2H*	*$\delta^{18}O$*	*δ^2H*
Jumandy station	−0.02	−0.01	−0.19	−0.39*	−0.38*	−0.12	−0.13
Ikiam station	−0.05	−0.07	−0.45**	−0.51**	−0.50**	−0.04	−0.05

* Denotes significant p-value < 0.05.
** Denotes significant p-value < 0.01.

during the monitoring period was 12.7 ‰. The highest monthly values were measured from July to September (13.9, 15.6, and 14.8 ‰). The lowest values were measured from April to May (10.7 and 11.0 ‰) and from December to January (9.8 and 10.9 ‰).

4.2. Stable isotopic composition of cave drip waters

The $\delta^{18}O$ drip-water values ranged from −6.8 to −6.3 (‰) for DW1, and from −6.9 to −6.3 (‰) for DW2. The $\delta^{2}H$ ranged from −41.9 to −40.3 (‰) for DW1, and from −42.6 to −40.6 (‰) for DW2. The average value of weekly $\delta^{18}O$ drip-water was −6.6 and −6.7 (‰) for the sites DW1 and DW2, respectively, while the values of $\delta^{2}H$ were −41.0 and −41.6 (‰) for DW1 and DW2, respectively. This average difference of 0.1 ‰ for $\delta^{18}O$ is on the order of the analytical precision, while the $\delta^{2}H$ is higher (0.5 ‰). This indicates that there were no strong local effects altering the $\delta^{18}O$ signature between the two monitoring sites. The reasonable variability of mean values together with the low amplitude of $\delta^{18}O$ and $\delta^{2}H$ values for drip-water values eliminates the possibility of strong evaporation of meteoric water along with the percolation of the water inside the cave. Therefore, it is likely that the O^{18} values of precipitation are well preserved in the drips that precipitate and form speleothems.

The discharge characteristics differ at the two monitoring dripping sites (DW1 and DW2) within the same cave. The dripping discharge rate ranged from 3.66 to 11.60 (mL/h) for DW1 at dripping site 1 (Fig. 6) and from 6.07 to 6.97 (mL/h) for DW2 at dripping site 2 (Fig. 7), and the average rate collected weekly was 7.71 and 6.56 (mL/h) respectively. At DW1, rainfall measurements recorded a peak in the last week of May (Fig. 6A), which is reflected three weeks later in the depleted $\delta^{18}O$ drip-water values (Fig. 6B). Likewise, in the first week of June precipitation decreases, and three weeks later an increase of $\delta^{18}O$ drip-water values is observed (Fig. 6C). AtDW2, the correspondence between the increase in precipitation during the last week of May and the depletion of $\delta^{18}O$ in the first week of June is more clearly observed (Fig. 7). The slightly inverse response three weeks after each event indicates a negative correlation between the two parameters. The behavior of dripping water is related to the intensity of the events since, after an intense event, part of the water infiltrates and the rest contributes to runoff. If these events are repetitive, the water saturates the epikarst, favoring infiltration. This is what happens in the Jumandy cave, mainly at DW2, where the drip volume responds relatively quickly in a way that is typical of caves with a shallow epikarst.

The average epikarst is 8.6 m, and the strata that constitute the vadose zone consist of unconsolidated material, limestone rocks, highly fractured limestone rocks, and limestone bedrock (Rivera, 2022). The cave is located in a tropical zone characterized by the presence of organic matter over the cave and high amounts of precipitation, which means that there is a high dissolution of the carbonate rocks that favor the conduits and fractures exist that allow a fast flow of water in the karst (Hu et al., 2015; Maloszewski et al., 2002). The discharge rates in both sites varied because after a precipitation event the hydraulic head increases within the karst, where the drip volume is dampened and redistributed due to the complexity of the karstic system (Tooth and Fairchild, 2003). The $\delta^{18}O$ and $\delta^{2}H$ values for drip-water compared to the rainfall signature (Figs. 6 and 7) and drip-water values plotted over the LMWLs (Fig. 5), confirms water and (therefore) isotopic mixing in

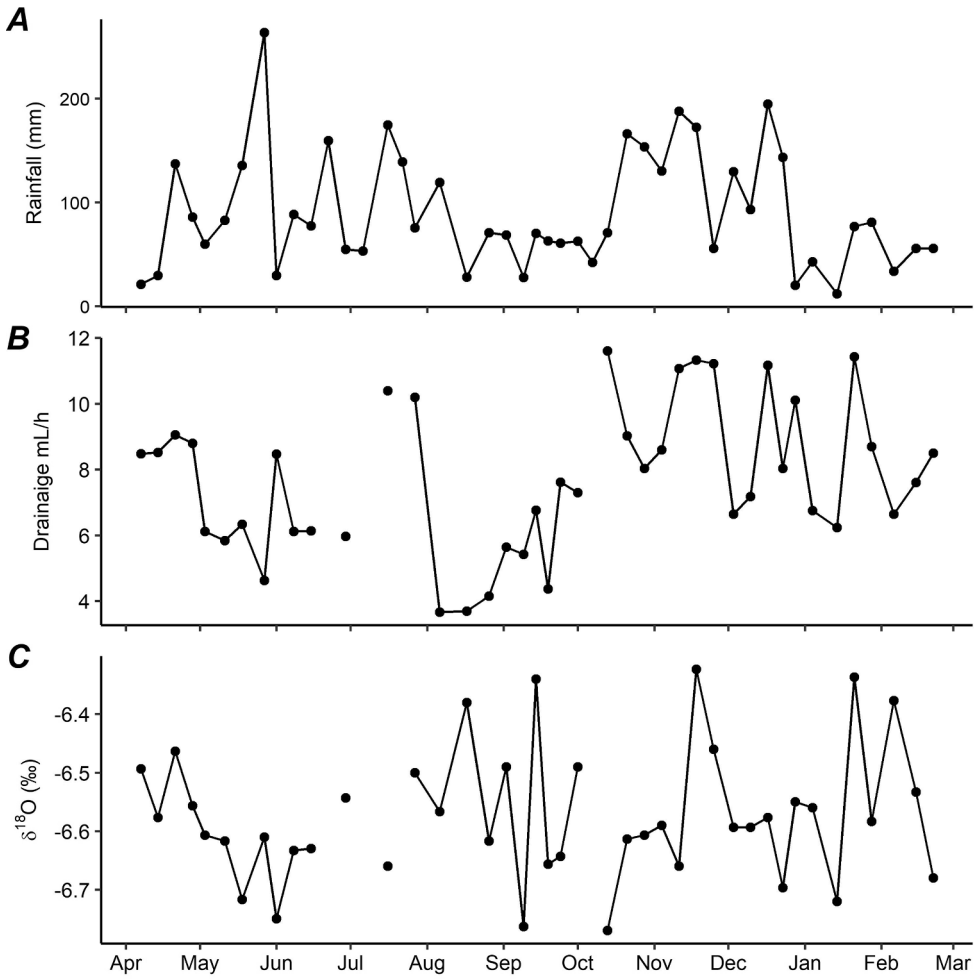

Fig. 6. Characteristics of the weekly drip water at site 1. A) Weekly rainfall amount. B) Dripping discharge rate. C) $\delta^{18}O$ values.

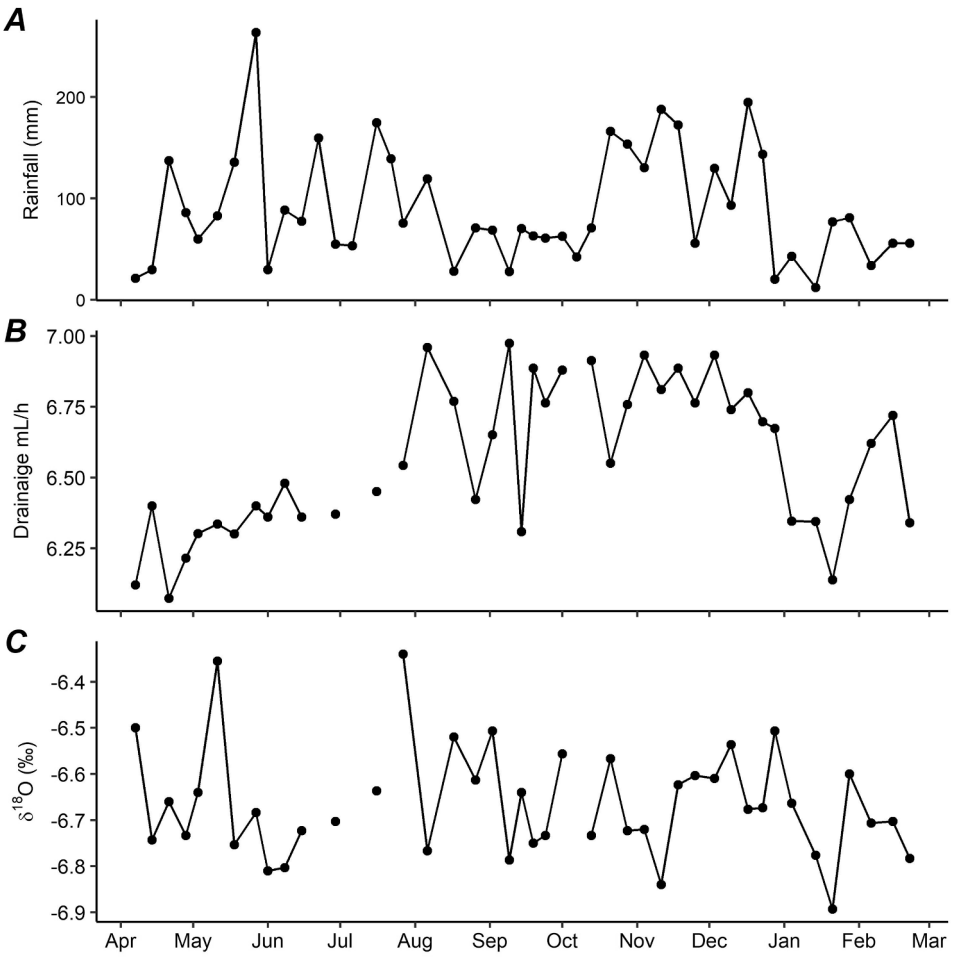

Fig. 7. Characteristics of the weekly drip water at site 2. A) Weekly rainfall amount. B) Dripping discharge rate. C) $\delta^{18}O$ values.

the epikarst. This result was expected because the drip-water isotopic signature results from multiple precipitation events that supply water that is mixed within the epikarst (Bar-Matthews et al., 1996; Cruz et al., 2005). Caves with a shallow epikarst are generally ideal for high-resolution paleoclimatic studies since the water infiltrated into the soil and vadose zone experiences shorter residence times (Cruz et al., 2009; Strikis et al., 2011).

The d-excess is a useful parameter to check if evaporation is occurring as water percolates through a karst aquifer (Dansgaard, 1964). The d-excess of drip-water ranged from 9.8 to 13.3 (‰) at DW1, and from 10.0 to 13.5 (‰) at DW2. The average values of d-excess were 11.6 and 11.8 (‰) similar to the rainfall values of Ikiam and Jumandy stations (Fig. 3E), which indicates absence of evaporation during water seepage through the soil and epikarst. Evaporation within the cave associated with low relative humidity could also affect the d-excess measured in the drip water, however, evaporation is negligible in Jumandy cave where temperature fluctuations are minimal year-round (ranging from 22.46 to 22.82 °C at site 1 and from 22.58 to 23.13 °C at site 2) and relative humidity always remained at 100 %. It also indicates optimal conditions for paleoclimatic studies based on speleothem isotope records.

The isotope values from the river drainages at WF1 ranged from −7.2 to −6.1 (‰) for $\delta^{18}O$ and −44.5 to −38.9 (‰) for $\delta^{2}H$. At WF2 they ranged from −7.0 to −5.2 (‰) for $\delta^{18}O$ and from −45.2 to −31.6 (‰) for $\delta^{2}H$. The average $\delta^{18}O$ values of water from river drainages were −6.6 ‰ at WF1 and −6.5 ‰ at WF2. The average $\delta^{2}H$ values were −41.7 ‰ at WF1 and −40.1 at WF2. $\delta^{18}O$ values from the cave waters, covary between the two monitoring points considering the analytical uncertainties (0.1 ‰). The correlation between isotopic composition of rainfall and river drainages for WF1 is weak and non-significant ($\rho = 0.08$; p-value = 0.62) whereas at WF2 the correlation is strong and significant ($\rho = 0.53$; p-value < 0.01). These results are consistent with the idea of higher transmissibility of water that percolates the main drainage of the cave (WF2) that is more directly fed by rainfall by conduit porosity, while its tributary receives a significant contribution from water from a fissured aquifer that accumulates in the vadose zone. In Fig. 5, this is evident as WF2 values are dispersed in the LMWLs (susceptible to fractionation processes greater than stored water in the epikarst) in response to the fast infiltration. Also, there was a significant correlation at 99 % between rainfall amount and the water level inside the cave, as well as rainfall and water flow. The weekly hydrograph depicted in Fig. 8, corroborates that the behavior of the flow inside the cave showed an instantaneous response following a precipitation event.

4.3. *Variability of moisture sources*

In this section, the dynamical aspects of moisture transport that characterize the precipitation $\delta^{18}O$ signature areassessed through wind back-trajectory analyses using the HYSPLIT model (e.g., Ampuero et al., 2020; Fiorella et al., 2015). In addition, composite maps of vertically integrated moisture-flux and rainfall anomalies are computed considering each cluster of the back-trajectories. Overall, $\delta^{18}O$ of rainfall showed a stronger correlation with DRU ($r = -0.55$, $p < 0.01$), than with local precipitation ($r = -0.41$, $p < 0.01$) during the monitoring period (Supplementary material: Table A.5). In the different seasons, the isotopic signature of tropical rainfall is influenced by the origin of air masses (moisture source effect) (Villacís et al., 2008). The results

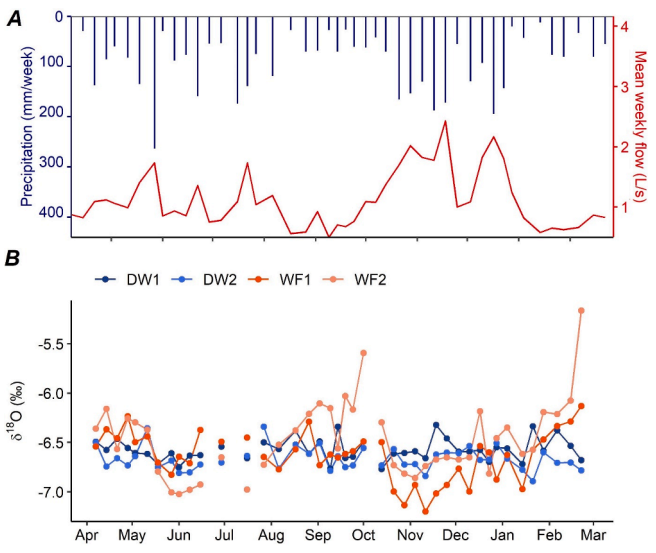

Fig. 8. Weekly hydrograph related to $\delta^{18}O$ values inside the cave. A) The flow of cave drainage water (red line) with respect to precipitation (blue bars). The cave is recharged directly by rainfall. B) Weekly ^{18}O values of drip water at site 1 (DW1, dark blue dot-line) and at site 2 (DW2, light blue dot-line) and water from river drainages at site 1 (WF1, orange-red dot-line) and at site 2 (WF2, pink dot-line). The figure provides evidence of rapid water entry into the karst system.

confirm that air masses that reach the study site represent a combination of large-scale moisture transport and local sources (Fig. 9). Large-scale atmospheric circulation transports moisture originating primarily over the Atlantic Ocean and passing through the Amazon Basin, following mainly pathways from the northeast, east and southeast. Local moisture sources are mainly associated with Mesoscale Convective Complexes (MCC) (Fig. 9).

From December 2019 to February 2020, local sources associated with cluster 3 (C3) are the most important for precipitation at the study site (Fig. 10D). In fact, this period was marked by a drought in southern Brazil, caused by a regional reduction of the moisture flux over the continent and other large-scale processes (Gomes et al., 2021). This is also evident in the composite analysis of precipitation, which does not show large-scale systems organizing convection in C3, and shows pervasive negative precipitation anomalies in the Amazon in all clusters (Fig. A.4). Northeastern, eastern and southeastern sources (C1, C4, C5 and C6) also appear but their contributions to precipitation are small. Moreover, DRU shows low values throughout this period (Fig. 10D). Consequently, $\delta^{18}O$ of precipitation during this season was the highest recorded (−4.75 ‰) (Supplementary material: Table A.6).

From April to May 2019, the main transport pathways are local, represented by C1 and C3, and from the northeast, represented by C4 (Fig. 10A). As this is a transition period, it is expected that rainfall is largely related to Mesoscale Convective Systems (MCSs). Moreover, composites also show large-scale moisture transport from east to west (Fig. A.4), and there is a very high DRU value associated with C4 (Fig. 10A). Convection related to the Intertropical Convergence Zone (ITCZ) landward extension and associated upstream rainout along the transport pathway (Villacís et al., 2008) lead to the most negative $\delta^{18}O$ of rainfall observed during the monitoring (−11.73 ‰) (Supplementary material: Table A.6).

From June to August 2019, the most frequent trajectories are local, represented by C1 and C3, and from the southeast, represented by C2 (Fig. 10B). Large-scale moisture transport from the southeast and east (Fig. A.4) are characterized by a lower depth of the trade winds, where the wind speeds decrease. Conversely, DRU values of the most important clusters are low. Hence, $\delta^{18}O$ values of rainfall at the study site are influenced by DRU, local moisture sources and evapotranspiration over the Amazon Basin. Consequently, the $\delta^{18}O$ mean is relatively low (−6.12 ‰) (Supplementary material: Table A.6). The d-excess of local rainfall is the highest during this period (14.65 ‰), coherent with the moisture flux pathways. Higher values of d-excess (>15) occur from July to September, peaking in July and August, when the frequency of moisture flux originating in the Amazon Basin is higher compared to the rest of the monitored time series. This relationship supports the notion that d-excess from the Amazon reflects the relative contribution of large-scale moisture recycling to precipitation at the study site (Ampuero et al., 2020).

Finally, from September to November 2019, the second transition season the most frequent back-trajectories are related to local sources represented by C3, and northeastern sources represented by C4 (Fig. 10B). DRU values remain low in all clusters. Under these conditions, $\delta^{18}O$ is relatively low (−6.30 ‰) (Supplementary material: Table A.6).

Although there are few back-trajectories originating in the Pacific Ocean (C3 and C1), significant moisture contributions from the Pacific to the study site are not likely under normal conditions. As air masses from the Pacific reach the Andes, the orographic lift leads to cooling, condensation and rainout over the western slope of the Andes. Once the air masses descend on the eastern side and reach the study site, the moisture content is too low to contribute significantly to precipitation. In order for water vapor to cross the Andes from west to east, favorable conditions with anomalously warm sea surface temperature (SST) in the Pacific region linked to the weakening of the trade winds (i.e., El Niño events) are necessary (Mayta et al., 2018). Hence it is unlikely that the Pacific is a significant moisture source for the study site during the monitoring period, although further monitoring should confirm this

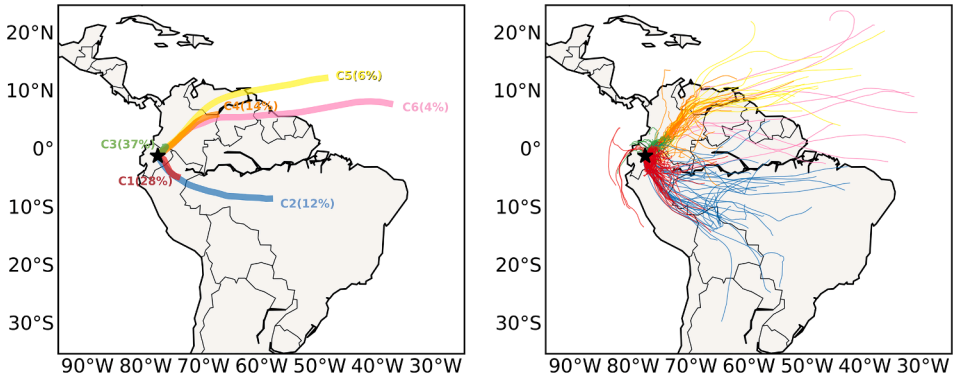

Fig. 9. Seven-day back-trajectories starting at the Ikiam station (star), at 1000 m above ground level (~730 hPa), from April 2019 to February 2020, considering only back-trajectories starting on precipitation days. The panel on the left shows the average path with the frequency of back-trajectories in percentage for each cluster, and the one on the right shows all back-trajectories.

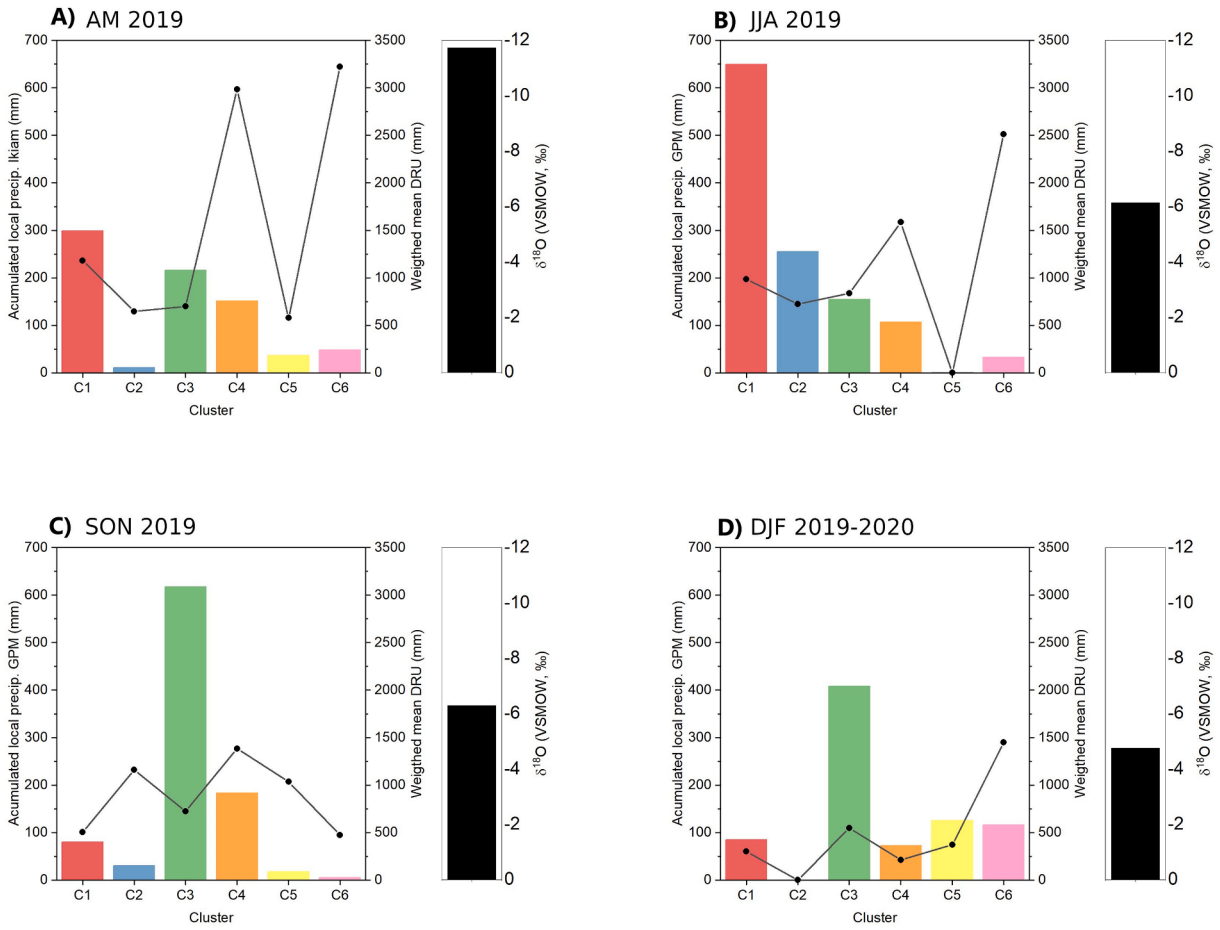

Fig. 10. Precipitation, DRU and $\delta^{18}O$ associated with each cluster of back-trajectories per season during the monitoring period. Accumulated precipitation (colored bars), weighted mean DRU (line with dots) and weighted mean $\delta^{18}O$ (black bar) for A) April - May 2019; B) June - July - August 2019; C) September - October - November 2019; and D) December 2019 - January - February 2020.

hypothesis. Rainfall during these periods is associated with moisture transport originating over the tropical Atlantic, mixing with evapotranspiration in the Amazon and local moisture.

5. Conclusions

The LMWLs of rainfall at the Jumandy and Ikiam stations, plot on top of the GMWL. The isotopic composition of precipitation shows a seasonal cycle, varying with the moisture transport patterns resulting from a combination of meso and large-scale convective systems. The isotopic values and the calculated back-trajectories confirm that the water vapor precipitating over the cave site presents the lowest $\delta^{18}O$ values in austral autumn, which reflects the strong convection associated with upstream rainout along the transport pathway, originating principally over the landward extension of ITCZ region. The significant recycling of moisture that occurs over the Amazon Basin influences the isotopic composition of rainfall as indicated by the d-excess, with maximum values during austral winter. These results are consistent with rainfall isotopic values reported by other studies in the region.

The two dripping sites inside the cave present different discharge characteristics. However, the isotopic signature of drip-water in both sites is similar. This means that the isotopic signature of the drip-water is buffered within the karst system and the drip-water represents a mixture of precipitation from multiple rainfall events. It is suggested that the storage time of the water within the epikarst is three weeks, typical of caves with shallow epikarst. However, confirming this hypothesis would require a longer monitoring period. On the other hand, isotopic values and hydrological response of water from river drainages allow us to conclude that the Jumandy cave, mainly site WF2, is fed directly by rainfall at a local scale. Thus, the Jumandy cave has fractures in the transmission zone that allow the continuous flow of water into the cave and small fissures where the water seeps into the subsoil and trickles into the epikarst.

Uncited references

CRediT authorship contribution statement

Angie Jiménez-Iñiguez: Formal analysis, Investigation, Data curation, Writing – original draft. **Angela Ampuero:** Formal analysis, Visualization, Data curation, Writing – original draft. **Bryan G. Valencia:** Conceptualization, Methodology, Writing – original draft. **Victor C. Mayta:** Visualization, Data curation, Writing – original draft. **Francisco W. Cruz:** Methodology, Writing – original draft. **Mathias Vuille:** Writing – review & editing. **Valdir F. Novello:** Writing – review & editing. **Nicolás Misailidis Stríkis:** Writing – review & editing. **Nataly Aranda:** Writing – review & editing. **Bruno Conicelli:** Writing – review & editing, Conceptualization, Methodology, Supervision, Project administration.

Declaration of Competing Interest

The authors declare the following financial interests/personal relationships which may be considered as potential competing interests: Bruno Conicelli reports financial support was provided by Amazon Regional University IKIAM.

Acknowledgements

This project was supported by the PIRE project (Climate Research and Education in the Americas using Tree-ring and speleothem Examples). We are grateful to the Ruku Jumandy Kawsay community for access to the cave, to Laboratorio Nacional de Referencia del Agua (LNRA), and all persons involved in the field and the lab work. We thank the two reviewers for their insightful suggestions that improved the manuscript.

Appendix A. Supplementary data

Supplementary data to this article can be found online at https://doi.org/10.1016/j.jhydrol.2022.127848.

References

Aggarwal, P.K., Romatschke, U., Araguas-Araguas, L., Belachew, D., Longstaffe, F.J., Berg, P., Schumacher, C., Funk, A., 2016. Proportions of convective and stratiform precipitation revealed in water isotope ratios. Nat. Geosci. 9, 624–629. https://doi.org/10.1038/ngeo2739.

Ampuero, A., Stríkis, N.M., Apaéstegui, J., Vuille, M., Novello, V.F., Espinoza, J.C., Cruz, F.W., Vonhof, H., Mayta, V.C., Martins, V.T.S., Cordeiro, R.C., Azevedo, V., Sifeddine, A., 2020. The Forest Effects on the Isotopic Composition of Rainfall in the Northwestern Amazon Basin. e2019JD031445 J. Geophys. Res.: Atmos. 125. https://doi.org/10.1029/2019jd031445.

Araguás-Araguás, L., Froehlich, K., Rozanski, K., 2000. Deuterium and oxygen-18 isotope composition of precipitation and atmospheric moisture. Hydrol. Process. 14, 1341–1355. https://doi.org/10.1002/1099-1085(20000615)14:8<1341::AID-HYP983>3.3.CO;2-Q.

Bar-Matthews, M., Ayalon, A., Mathews, A., Sass, A., Halicz, L., 1996. Carbon and oxygen isotope study of the active water-carbonate system in a karstic Mediterranean cave: Implications for paleoclimate research in semiarid regions. Geochim. Cosmochim. Acta 60, 337–347. https://doi.org/10.1016/0016-7037(95)00395-9.

Bauz, R., Mena, E., 2015. Revista sobre la biodiversidad y el ecoturismo de las Cavernas de Jumandy, en el cantón Archidona en la Provincia de Napo-Tena. (Bachelor's theses). Universidad Regional Amazónica Ikiam, Napo.

Campos, J.L.P.S., Cruz, F.W., Ambrizzi, T., Deininger, M., Vuille, M., Novello, V.F., Strikis, N.M., 2019. Coherent South American Monsoon variability during the last millennium revealed through high-resolution proxy records. Geophys. Res. Lett. 46, 8261–8270. https://doi.org/10.1029/2019GL082513.

Chapman, J.B., Ingraham, N.L., Hess, J.W., 1992. Isotopic investigation of infiltration and unsaturated zone flow processes at Carlsbad Cavern, New Mexico. J. Hydrol. 133, 343–363. https://doi.org/10.1016/0022-1694(92)90262-T.

Cheng, H., Sinha, A., Cruz, F.W., Wang, X., Edwards, R.L., d'Horta, F.M., et al., 2013. Climate change patterns in Amazonia and biodiversity. Nat. Commun. 4, 1411. https://doi.org/10.1038/ncomms2415.

Clark, I., 2015. Groundwater Geochemistry and Isotopes. Groundwater 53, 832–833. https://doi.org/10.1111/gwat.12377.

Cobb, K.M., Adkins, J.F., Partin, J.W., Clark, B., 2007. Regional-scale climate influences on temporal variations of rainwater and cave dripwater oxygen isotopes in northern Borneo. Earth Planet. Sci. Lett. 263, 207–220. https://doi.org/10.1016/j.epsl.2007.08.024.

Constantin, S., Toulkeridis, T., Moldovan, O.T., Addison, A., Constantin, S., Toulkeridis, T., Moldovan, O.T., 2018. Caves and karst of Ecuador – state-of-the-art and research perspectives. Phys. Geogr. 3646, 1–24. https://doi.org/10.1080/02723646.2018.1461496.

Craig, H., Gordon, L.I., 1965. Deuterium and oxygen 18 variations in the ocean and the marine atmosphere.

Cruz, F.W., Karmann, I., Viana, O., Burns, S.J., Ferrari, J.A., Vuille, M., Sial, A.N., Moreira, M.Z., 2005. Stable isotope study of cave percolation waters in subtropical Brazil: Implications for paleoclimate inferences from speleothems. Chem. Geol. 220 (3-4), 245–262.

Cruz, F.W., Vuille, M., Burns, S.J., Wang, X., Cheng, H., Werner, M., Edwards, R.L., Karmann, I., Auler, A.S., Nguyen, H., 2009. Orbitally driven east-west antiphasing of South American precipitation. Nat. Geosci. 2, 210–214. https://doi.org/10.1038/ngeo444.

Dansgaard, W., 1964. Stable isotopes in precipitation. Tellus 16, 436–468. https://doi.org/10.3402/tellusa.v16i4.8993.

Della Libera, M.E., Novello, V.F., Cruz, F.W., Orrison, R., Vuille, M., Maezumi, S.Y., de Souza, J., Cauhy, J., Campos, J.L.P.S., Ampuero, A., Utida, G., Stríkis, N.M., Stumpf, C.F., Azevedo, V., Zhang, H., Edwards, R.L., Cheng, H., 2022. Paleoclimatic and paleoenvironmental changes in Amazonian lowlands over the last three millennia. Quarter. Sci. Rev. 279, 107383.

Dhungana, R., Aharon, P., 2019. Stable isotopes and trace elements of drip waters at DeSoto Caverns during rainfall-contrasting years. Chem. Geol. 504, 96–104. https://doi.org/10.1016/j.chemgeo.2018.11.002.

Dreybrodt, W., Scholz, D., 2011. Climatic dependence of stable carbon and oxygen isotope signals recorded in speleothems: From soil water to speleothem calcite. Geochim. Cosmochim. Acta 75, 734–752. https://doi.org/10.1016/j.gca.2010.11.002.

Duan, W., Ruan, J., Luo, W., Li, T., Tian, L., Zeng, G., Zhang, D., Bai, Y., Li, J., Tao, T., Zhang, P., Baker, A., Tan, M., 2016. The transfer of seasonal isotopic variability between precipitation and drip water at eight caves in the monsoon regions of China. Geochim. Cosmochim. Acta 183, 250–266. https://doi.org/10.1016/j.gca.2016.03.037.

Espinoza, J.C., Guyot, J.L., Ronchail, J., Cochonneau, G., Filizola, N., Fraizy, P., Labat, D., de Oliveira, E., Ordoñez, J.J., Vauchel, P., 2009. Contrasting regional discharge evolutions in the Amazon basin (1974–2004). J. Hydrol. 375, 297–311. https://doi.org/10.1016/j.jhydrol.2009.03.004.

Esquivel-Hernández, G., Mosquera, G.M., Sánchez-Murillo, R., Quesada-Román, A., Birkel, C., Crespo, P., Célleri, R., Windhorst, D., Breuer, L., Boll, J., 2019. Moisture transport and seasonal variations in the stable isotopic composition of rainfall in Central American and Andean Páramo during El Niño conditions (2015–2016). Hydrol. Process. 33, 1802–1817. https://doi.org/10.1002/hyp.13438.

Estupiñan, J., Marfil, R., Scherer, M., Permanyer, A., 2010. Reservoir sandstones of the cretaceous napo formation U And T members in the oriente basin, ecuador: Links between diagenesis and sequence stratigraphy. J. Pet. Geol. 33, 221–245. https://doi.org/10.1111/j.1747-5457.2010.00475.x.

Tooth, A.F., Fairchild, I.J., 2003. Soil and karst aquifer hydrological controls on the geochemical evolution of speleothem-forming drip waters, Crag Cave, southwest Ireland. J. Hydrol. 273 (1-4), 51–68.

Fairchild, I.J., Tuckwell, G.W., Baker, A., Tooth, A.F., 2006. Modelling of dripwater hydrology and hydrogeochemistry in a weakly karstified aquifer (Bath, UK): Implications for climate change studies. J. Hydrol. 321, 213–231. https://doi.org/10.1016/j.jhydrol.2005.08.002.

Fiorella, R.P., Poulsen, C.J., Zolá, R.S.P., Barnes, J.B., Tabor, C.R., Ehlers, T.A., 2015. Erratum: Spatiotemporal variability of modern precipitation $\delta^{18}O$ in the central Andes and implications for paleoclimate and paleoaltimetry estimates. J. Geophys. Res. 120, 4630–4656. https://doi.org/10.1002/2014JD022893.

Froehlich, K., Gibson, J., Aggarwal, P.K., 2002. Deuterium excess in precipitation ans its climatological significance. IAEA 1000, 54–66.

Fuller, L., Baker, A., Fairchild, I.J., Spötl, C., Marca-Bell, A., Rowe, P., Dennis, P.F., 2008. Isotope hydrology of dripwaters in a Scottish cave and implications for stalagmite palaeoclimate research. Hydrol. Earth Syst. Sci. 12, 1065–1074. https://doi.org/10.5194/hess-12-1065-2008.

Garreaud, R.D., Vuille, M., Compagnucci, R., Marengo, J., 2009. Present-day South American climate. Palaeogeogr. Palaeoclimatol. Palaeoecol. 281, 180–195. https://doi.org/10.1016/j.palaeo.2007.10.032.

Gastmans, D., Santos, V., Galhardi, J.A., Gromboni, J.F., Batista, L.V., Miotlinski, K., Chang, H.K., Govone, J.S., 2017. Controls over spatial and seasonal variations on isotopic composition of the precipitation along the central and eastern portion of Brazil. Isotopes Environ. Health Stud. 53, 518–538. https://doi.org/10.1080/10256016.2017.1305376.

Gat, J.R., Matsui, E., 1991. Atmospheric water balance in the Amazon basin: An isotopic evapotranspiration model. J. Geophys. Res. 96, 13179–13188.

Gomes, M.S., Cavalcanti, I.F. de A., Müller, G.v., 2021. 2019/2020 drought impacts on South America and atmospheric and oceanic influences. Weather Clim. Extremes 34, 100404. https://doi.org/10.1016/j.wace.2021.100404.

Gonfiantini, R., Roche, M.-A., Olivry, J.-C., Fontes, J.-C., Zuppi, G.M., 2001. The altitude effect on the isotopic composition of tropical rains. Chem. Geol. 181 (1-4), 147–167.

Grootes, P., Stuiver, M., Thompson, L., Mosley-Thompson, E., 1989. Oxygen isotope changes in tropical ice, Quelccaya, Peru. J. Geophys. Res. 94, 1187–1194. https://doi.org/10.1029/JD094iD01p01187.

Hardy, D., Vuille, M., Bradley, R.S., 2003. Variability of snow accumulation and isotopic composition on Nevado Sajama, Bolivia. J. Geophys. Res. 108 (D22), 4693. https://doi.org/10.1029/2003JD003623.

Hastenrath, S., 1997. Annual cycle of upper air circulation and convective activity over the tropical Americas. Geophys. Res. 102 (D4), 4267–4274.

Hersbach, H., Bell, B., Berrisford, P., Biavati, G., Horányi, A., Muñoz Sabater, J., Nicolas, J., Peubey, C., Radu, R., Rozum, I., Schepers, D., Simmons, A., Soci, C., Dee, D., Thépaut, J-N., 2018a. ERA5 hourly data on pressure levels from 1979 to present. Copernicus Climate Change Service (C3S) Climate Data Store (CDS). (Accessed on 10-Jan-2022), 10.24381/cds.bd0915c6.

Hersbach, H., Bell, B., Berrisford, P., Biavati, G., Horányi, A., Muñoz Sabater, J., Nicolas, J., Peubey, C., Radu, R., Rozum, I., Schepers, D., Simmons, A., Soci, C., Dee, D., Thépaut, J-N., 2018b. ERA5 hourly data on single levels from 1979 to present. Copernicus Climate Change Service (C3S) Climate Data Store (CDS). (Accessed on < 10-Jan-2022 >), 10.24381/cds.adbb2d47.

Hoffmann, G., 2003. Taking the Pulse of the Tropical Water Cycle. Science (80-) 5201, 776–777. https://doi.org/10.1126/science.1085066.

Hoorn, C., Wesselingh, F.P., ter Steege, H., Bermudez, M.A., Mora, A., Sevink, J., Sanmartín, I., Sanchez-Meseguer, A., Anderson, C.L., Figueiredo, J.P., Jaramillo, C., Riff, D., Negri, F.R., Hooghiemstra, H., Lundberg, J., Stadler, T., Särkinen, T., Antonelli, A., 2010. Amazonia Through Time : Andean Uplitf, Climate Change, Landscape Evolution, and Biodiversity. Science (80-) 330, 927–931. https://doi.org/10.1126/science.1194585.

Hu, K., Chen, H., Nie, Y., Wang, K., 2015. Seasonal recharge and mean residence times of soil and epikarst water in a small karst catchment of southwest China. Scientific reports, 5(1), 1–12. Huffman, G.J., Bolvin, D.T., Braithwaite, D., Hsu, K.L., Joyce, R. J., Kidd, C., Nelkin, E.J., Sorooshian, S., Stocker, E.F., Tan, J., Wolff, D.B., Xie, P., 2020. Integrated Multi-satellite Retrievals for the Global Precipitation Measurement (GPM) Mission (IMERG). Adv. Glob. Chang. Res. 67, 343–353. https://doi.org/10.1007/978-3-030-24568-9_19.

Hurley, J.V., Vuille, M., Hardy, D.R., Burns, S., Thompson, L.G., 2015. Cold air incursions, $\delta^{18}O$ variability and monsoon dynamics associated with snow days at

Quelccaya Ice Cap, Peru. J. Geophys. Res., 120, 7467–7487. https://doi.org/10.109/2015JD023323.
Hurley, J.V., Vuille, M., Hardy, D.R., 2016. Forward modeling of ^{18}O in Andean ice cores. Geophys. Res. Lett. 43 (15), 8178–8188. https://doi.org/10.1002/2016GL070150.
IAEA/WMO, 2014. Global network of isotopes in precipitation. The GNIP Database 19.
Kanner, L.C., Burns, S.J., Cheng, H., Edwards, R.L., Vuille, M., 2013. High-resolution variability of the South American summer monsoon over the last seven millennia: Insights from a speleothem record from the central Peruvian Andes. Quat. Sci. Rev. 75, 1–10. https://doi.org/10.1016/j.quascirev.2013.05.008.
Lachniet, M., 2009. Climatic anf Environmental Controls on Speleothem Oxygen Isotope Values. Quarter. Sci. Rev. 28, 412–432.
Lambert, J., Aharon, P., 2010. Oxygen and hydrogen isotopes of rainfall and dripwater at DeSoto Caverns (Alabama, USA): Key to understanding past variability of moisture transport from the Gulf of Mexico. Geochim. Cosmochim. Acta 74, 846–861. https://doi.org/10.1016/j.gca.2009.10.043.
Lee, J.E., Johnson, K., Fung, I., 2009. Precipitation over South America during the Last Glacial Maximum: an analysis of the "amount effect" with a water isotope-enabled general circulation model. Geophys. Res. Lett. 36, L19701. https://doi.org/10.1029/2009GL039265, 2009.
Luo, W., Wang, S., Xie, X., 2013. A comparative study on the stable isotopes from precipitation to speleothem in four caves of Guizhou, China. Chemie der Erde 73, 205–215. https://doi.org/10.1016/j.chemer.2012.05.002.
Maloszewski, P., Stichler, W., Zuber, A., Rank, D., 2002. Identifying the flow systems in a karstic-fissured-porous aquifer, the Schneealpe, Austria, by modelling of environmental 18O and 3 H isotopes. J. Hydrol. 256, 48–59. https://doi.org/10.1016/S0022-1694(01)00526-1.
Martinelli, L.A., Victoria, R.L., Sternberg, L.S.L., Ribeiro, A., Moreira, M.Z., 1996. Using stable isotopes to determine sources of evaporated water to the atmosphere in the Amazon basin. J. Hydrol. 183, 191–204. https://doi.org/10.1016/0022-1694(95)02974-5.
Matthews, A., Ayalon, A., Bar-Matthews, M., 2000. D/H ratios of fluid inclusions of Soreq cave (Israel) speleothems as a guide to the Eastern Mediaterranean Meteoric Line relationships in the last 120 ky. Chem. Geol. 166, 183–191. https://doi.org/10.1016/S0009-2541(99)00192-8.
Mayta, V.C., Ambrizzi, T., Espinoza, J.C., Silva Dias, P.L., 2018. The role of the Madden–Julian oscillation on the Amazon Basin intraseasonal rainfall variability. Int. J. Climatol. 39, 343–360. https://doi.org/10.1002/joc.5810.
Moquet, J.S., Cruz, F.W., Novello, V.F., Stríkis, N.M., Deininger, M., Karmann, I., Santos, R.V., Millo, C., Apaestegui, J., Guyot, J.L., Siffedine, A., Vuille, M., Cheng, H., Edwards, R.L., Santini, W., 2016. Calibration of speleothem δ18O records against hydroclimate instrumental records in Central Brazil. Glob. Planet. Change 139, 151–164. https://doi.org/10.1016/j.gloplacha.2016.02.001.
Mosblech, N.A.S., Bush, M.B., Gosling, W.D., Hodell, D., Thomas, L., Van Calsteren, P., Correa-Metrio, A., Valencia, B.G., Curtis, J., Van Woesik, R., 2012. North Atlantic forcing of Amazonian precipitation during the last ice age. Nat. Geosci. 5, 817–820. https://doi.org/10.1038/ngeo1588.
Munksgaard, N.C., Kurita, N., Sánchez-Murillo, R., Ahmed, N., Araguas, L., Balachew, D. L., Bird, M.I., Chakraborty, S., Kien Chinh, N., Cobb, K.M., Ellis, S.A., Esquivel-Hernández, G., Ganyaglo, S.Y., Gao, J., Gastmans, D., Kaseke, K.F., Kebede, S., Morales, M.R., Mueller, M., Poh, S.C., dos Santos, V., Shaoneng, H., Wang, L., Yacobaccio, H., Zwart, C., 2019. Data Descriptor: Daily observations of stable isotope ratios of rainfall in the tropics. Sci. Rep. 9, 1–7. https://doi.org/10.1038/s41598-019-50973-9.
Polk, J.S., van Beynen, P., Wynn, J., 2012. An isotopic calibration study of precipitation, cave dripwater, and climate in west-central Florida. Hydrol. Process. 26, 652–662. https://doi.org/10.1002/hyp.8169.
Risi, C., Bony, S., Vimeux, F., 2008. Influence of convective processes on the isotopic composition (δ18O and δD) of precipitation and water vapor in the tropics: 2. Physical interpretation of the amount effect. J. Geophys. Res. Atmos. 113, 1–12. https://doi.org/10.1029/2008JD009943.
Rivera, H., 2022. Identificación del epikarst en las Cavernas Humanti mediante refracción sísmica, (Bachelor's theses). Universidad Regional Amazónica Ikiam, Napo.
Rolph, G., Stein, A., Stunder, B., 2017. Real-time Environmental Applications and Display sYstem: READY. Environ. Model. Softw. 95, 210–228. https://doi.org/10.1016/j.envsoft.2017.06.025.
Rozanski, K., Araguás-Araguás, L., Gonfiantini, R., 1993. Isotopic Patterns in Modern Global Precipitation. Climate Change in Continental Isotopic Records. , AGU Geophys. 1–36 https://doi.org/10.1029/GM078p0001.
Rozanski, K., Johnsen, S.J., Schotterer, U., Thompson, L.G., 1997. Reconstruction of past climates from stable isotope records of palaeo-precipitation preserved in continental archives. Hydrol. Sci. J. 42, 725–745. https://doi.org/10.1080/02626669709492069.
Salati, E., Dall'Olio, A., Matsui, E., Gat, J.R., 1979. Recycling of water in the Amazon Basin: An isotopic study. Water Resour. Res. 15 (5), 1250–1258.
Sánchez, J., Zurita, M., Schwarz, A., Cárdenas, V.,Bonilla, J., Quilumba, D., et al., 2017. Guía Espeleológica de la Provincia de Napo.
Souza, E., Galvão, P., de Almeida, R., Pinheiro, C., Bessa, M., Cabral, M., 2015. Stable Isotopes Studies in the Urucu Oil Province, Amazon Region, Brazzil. J. Water Resour. Protect. 7, 131–142. https://doi.org/10.4236/jwarp.2015.73011.
Staal, A., Tuinenburg, O.A., Bosmans, J.H.C., Holmgren, M., Van Nes, E.H., Scheffer, M., Zemp, D.C., Dekker, S.C., 2018. Forest-rainfall cascades buffer against drought across the Amazon. Nat. Clim. Chang. 8, 539–543. https://doi.org/10.1038/s41558-018-0177-y.
Stein, A.F., Ngan, F., Draxler, R.R., Chai, T., 2015. Potential Use of Transport and Dispersion Model Ensembles for Forecasting Applications. Weather Forecast. 30, 639–655. https://doi.org/10.1175/WAF-D-14-00153.1.
Strikis, N.M., Cruz, F.W., Cheng, H., Karmann, I., Edwards, R.L., Vuille, M., Wang, X., de Paula, M.S., Novello, V.F., Auler, A.S., 2011. Abrupt variations in South American monsoon rainfall during the Holocene based on a speleothem record from central-eastern Brazil. Geology 39 (11), 1075–1078.
Villacís, M., Vimeux, F., Taupin, J.D., 2008. Analysis of the climate controls on the isotopic composition of precipitation (δ18O) at Nuevo Rocafuerte, 74.5°W, 0.9°S, 250 m, Ecuador. Comptes Rendus - Geosci. 340, 1–9. https://doi.org/10.1016/j.crte.2007.11.003.
Vimeux, F., Gallaire, R., Bony, S., Hoffmann, G., Chiang, J.C.H., 2005. What are the climate controls on δD in precipitation in the Zongo Valley (Bolivia)? Implications for the Illimani ice core interpretation. Earth Planet. Sci. Lett. 240, 205–220. https://doi.org/10.1016/j.epsl.2005.09.031.
Vuille, M., Bradley, R.S., Werner, M., Healy, R., Keimig, F., 2003. Modeling δ18O in Precipitation over the Tropical Americas: Interannual Variability and Climatic Controls. J. Geophys. Res. 108 (D6), 4174. https://doi.org/10.1029/2001JD002038.
Vuille, M., Werner, M., 2005. Stable isotopes in precipitation recording South American summer monsoon and ENSO variability: Observations and model results. Clim. Dyn. 25, 401–413. https://doi.org/10.1007/s00382-005-0049-9.
Vuille, M., Burns, S.J., Taylor, B.L., Cruz, F.W., Bird, B.W., Abbott, M.B., Kanner, L.C., Cheng, H., Novello, V.F., 2012. A review of the South American monsoon history as recorded in stable isotopic proxies over the past two millennia. Clim. Past 8, 1309–1321. https://doi.org/10.5194/cp-8-1309-2012.
Vuille, M., 2018. Current state and future challenges in stable isotope applications of the tropical hydrologic cycle (Invited Commentary). Hydrol. Process. 32, 1313–1317. https://doi.org/10.1002/hyp.11490.
Wainer, K., Genty, D., Blamart, D., Daëron, M., Bar-Matthews, M., Vonhof, H., Dublyansky, Y., Pons-Branchu, E., Thomas, L., van Calsteren, P., Quinif, Y., Caillon, N., 2011. Speleothem record of the last 180 ka in Villars cave (SW France): Investigation of a large δ18O shift between MIS6 and MIS5. Quat. Sci. Rev. 30, 130–146. https://doi.org/10.1016/j.quascirev.2010.07.004.
Wang, X., Edwards, R.L., Auler, A.S., Cheng, H., Kong, X., Wang, Y., Cruz, F.W., Dorale, J. A., Chiang, H.W., 2017. Hydroclimate changes across the Amazon lowlands over the past 45,000 years. Nature 541, 204–207. https://doi.org/10.1038/nature20787.
Williams, P.W., Fowler, A., 2002. Relationship between oxygen isotopes in rainfall, cave percolation waters and speleothem calcite at Waitomo, New Zealand. J. Hydrol. New Zeal.
Windhorst, D., Waltz, T., Timbe, E., Frede, H.G., Breuer, L., 2013. Impact of elevation and weather patterns on the isotopic composition of precipitation in a tropical montane rainforest. Hydrol. Earth Syst. Sci. 17, 409–419. https://doi.org/10.5194/hess-17-409-2013.
Yonge, C.J., Ford, D.C., Gray, J., Schwarcz, H.P., 1985. Stable isotope studies of cave seepage water. Chem. Geol. Isot. Geosci. Sect. 58, 97–105. https://doi.org/10.1016/0168-9622(85)90030-2.